JACS
JOURNAL OF THE AMERICAN CHEMICAL SOCIETY

ARTICLE

pubs.acs.org/JACS

Disappearance and Recovery of Luminescence in Bi^{3+}, Eu^{3+} Codoped YPO_4 Nanoparticles Due to the Presence of Water Molecules Up to 800 °C

M. Niraj Luwang,[†] R. S. Ningthoujam,*[,‡] S. K. Srivastava,[†] and R. K. Vatsa[‡]

[†]Department of Chemistry, Manipur University, Imphal-795003, India

[‡]Chemistry Division, Bhabha Atomic Research Center, Mumbai-400085, India

Supporting Information

ABSTRACT: YPO_4 nanoparticles codoped with Eu^{3+} (5 at. %) and Bi^{3+} (2−10 at. %) have been synthesized by a simple coprecipitation method using a polyethylene glycol−glycerol mixture, which acts as capping agent. It has been found that the incorporation of Bi^{3+} ions into the YPO_4:Eu^{3+} lattice induces a phase transformation from tetragonal to hexagonal, and also a significant decrease in Eu^{3+} luminescence intensity was observed. This is related to the association of the water molecules in the hexagonal phase of YPO_4 in which the nonradiative process from the surrounding water molecules around Eu^{3+} is dominating over the radiative process. On annealing above 800 °C, luminescence intensity recovers due to significant removal of water. 900 °C annealed Bi^{3+} codoped YPO_4:Eu^{3+} shows enhanced luminescence (2−3 times) as compared to that of YPO_4:Eu^{3+}. When sample was prepared in D_2O (instead of H_2O), 4-fold enhancement in luminescence was observed, suggesting the extent of reduction of multiphonon relaxation in D_2O. This study illustrates the stability of water molecules even at a very high temperature up to 800 °C in Eu^{3+} and Bi^{3+} codoped YPO_4 nanoparticles.

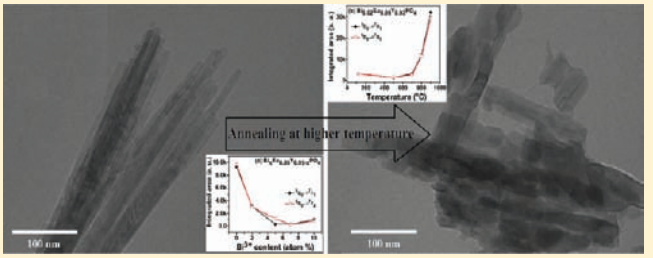

1. INTRODUCTION

Rare-earth phosphates ($REPO_4$) are used as a host in luminescence materials,[1] and the crystal structure of the $REPO_4$ changes from tetragonal to monoclinic as the ionic size of RE^{3+} increases.[1−3] However, hexagonal phase is formed irrespective of the ionic size of RE^{3+} if the water molecules (2−3) are associated in a unit cell during preparation, and this phase is stable even at higher temperature. This was reported in the hexagonal phase of $EuPO_4$ in which water molecules are stable up to 600 °C.[4] A similar observation was reported in other systems like $CuSO_4 \cdot 5H_2O$ in which water molecules are stable up to 200 °C.[5] Recently, our group (Ningthoujam and his co-workers)[2] found that water molecules can be retained up to 800 °C in hexagonal phase of Ce^{3+} codoped YPO_4:Eu^{3+}. If the water molecules are associated in the hexagonal phase, luminescence intensities are almost quenched.[2]

It has been reported that codoping of Bi^{3+} ions improves the luminescence intensity of RE^{3+} doped compounds such as Y_2O_3:Eu^{3+}, Bi^{3+}, $LnVO_4$:Eu^{3+}, Bi^{3+} on UV excitation.[6,7] This is because of the energy transfer from Bi^{3+} to the RE^{3+} ions. Bi^{3+} acts as sensitizer, whereas Eu^{3+} acts as activator. Bi^{3+} ions have the absorption peak at 330 nm and emission peak at 410 nm. In case of Eu^{3+} ions, the intensive absorption peak is obtained at 395 nm and emission peaks are at 591 and 617 nm, and because of this, Eu^{3+} doped compounds are used as red emitter in display and lighting applications.[8,9] The maximum energy transfer from Bi^{3+} to Eu^{3+} is possible if the nonradiative processes surrounding the Bi^{3+} is kept to a minimum. In addition to this, overlapping of electric dipole fields of sensitizer (emission) and activator (absorption) is also a major requirement for energy transfer. So, the role of Bi^{3+} in enhancement of luminescence in Eu^{3+} doped Y_2O_3 and $LnVO_4$ is still confusing. Could it be a case of energy transfer from Bi^{3+} to Eu^{3+} in the case of Bi^{3+} codoped YPO_4:Eu^{3+}? So far, there are no detailed studies in luminescence.

In this study, we found that luminescence intensity decreases with the increasing Bi^{3+} content in as-prepared YPO_4:Eu^{3+}. This is related to the association of the water molecules in the hexagonal phases of YPO_4 in which the nonradiative process from surrounding water molecules is dominating over the radiative process. Interestingly, luminescence intensity can be recovered after annealing above 800 °C at which the phase change from hexagonal to tetragonal structure takes place. Also, we observed that Bi^{3+} doping increases the luminescence intensity for the compounds annealed above 800 °C.

2. RESULTS AND DISCUSSION

2.1. XRD Study. Figure 1a shows the X-ray diffraction (XRD) patterns of as-synthesized pure YPO_4, $Eu_{0.05}Y_{0.95}PO_4$, and

Received: October 14, 2010
Published: February 10, 2011

   dx.doi.org/10.1021/ja1092437 | J. Am. Chem. Soc. 2011, 133, 2998–3004

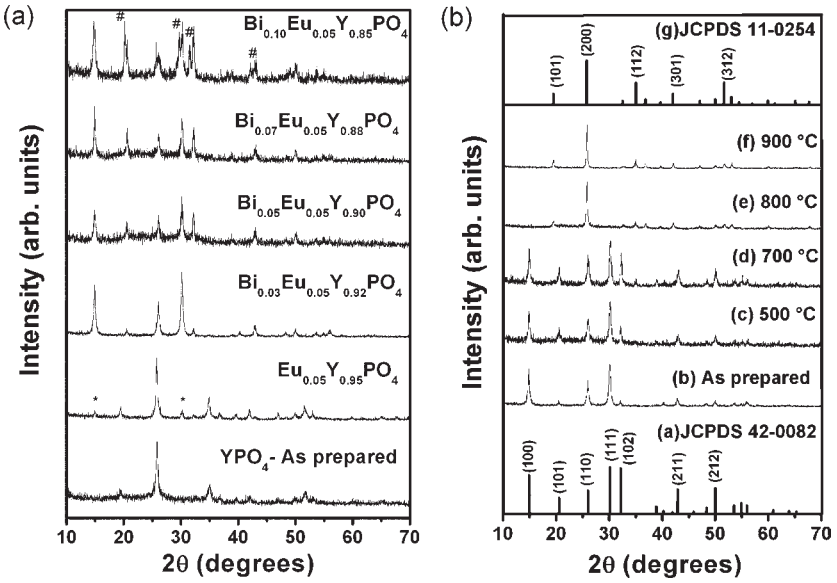

Figure 1. XRD patterns of (a) as-prepared samples of YPO_4 codoped with Eu^{3+} and Bi^{3+} and (b) $Bi_{0.02}Eu_{0.05}Y_{0.93}PO_4$ annealed at different annealing temperatures along with JCPDS card nos. 42-0082 (hexagonal) and 11-0254 (tetragonal). (Symbols "*" and "#" indicate the hexagonal phase of YPO_4 and $BiPO_4$, respectively.)

$Bi_xEu_{0.05}Y_{0.95-x}PO_4$ (x = 0.02, 0.05, 0.07, and 0.10). As-synthesized pure YPO_4 is well-crystalline tetragonal phase (JCPDS card no. 11-0254). The $Eu_{0.05}Y_{0.95}PO_4$ also shows a well-crystalline tetragonal system with extra diffraction peaks (marked by symbol "*"), while the Bi^{3+} codoped samples show a complete hexagonal phase (JCPDS card no. 42-0082). However, these extra peaks are weak as compared to those of the tetragonal phase. With the codoping of the Bi^{3+} ions, the tetragonal phase has been fully converted to the hexagonal phase. At higher codopant concentration of Bi^{3+} (10 at. %), additional hexagonal peaks relating to the $BiPO_4$ phase (JCPDS no. 45-1370) are observed (marked with symbol "#"). This result suggests that Bi^{3+} ions can be incorporated to YPO_4:Eu^{3+} up to a maximum of 7 at. % and above which, it leads to the formation of a new phase of $BiPO_4$ and also affects the luminescence intensity (as explained later). Based on the tetragonal structure, lattice parameters of pure YPO_4 are a = 6.897 and c = 6.037 Å. The lattice parameters, unit cell volume, and crystallite size calculated for all the samples are summarized in Table S1 (see the Supporting Information) along with the reported values of YPO_4 (JCPDS card no. 11-0254, tetragonal structure) and hydrated $YPO_4 \cdot 0.8H_2O$ (JCPDS card no. 42-0082, hexagonal structure). Unit cell volume increases slightly with Eu^{3+} or Bi^{3+} doping in YPO_4, which suggests the substitution of Y^{3+} (1.01 Å) ion by Eu^{3+} (1.07 Å) or Bi^{3+} (1.17 Å). The hexagonal phase contains water in hydrated form as $A_{0.05}Y_{0.95}PO_4$ (A = Eu^{3+} or Bi^{3+})$\cdot n H_2O$ ($YPO_4 \cdot 0.8H_2O$, JCPDS card no. 42-0082). Figure 1b shows the XRD diffraction pattern of $Bi_{0.02}Eu_{0.05}Y_{0.93}PO_4$ at different annealing temperatures along with the JCPDS card nos. 11-0254 and 42-0082. The as-prepared sample for the Bi^{3+} (2 at. %) codoped $Eu_{0.05}Y_{0.95}PO_4$ represents XRD patterns resembling the hydrated hexagonal phase of JCPDS card no. 42-0082. With the increase of the annealing temperature, the crystallinity increases for both the tetragonal and the hexagonal phases. The hexagonal phase transforms to a tetragonal phase at higher temperature (800 °C onward), which can be attributed to the dehydration of the hydrated hexagonal phase of YPO_4. In our previous work on the Ce^{3+} codoped YPO_4:Eu^{3+}, the phase transition from hexagonal to tetragonal structure was observed at an annealing temperature of 900 °C.[2] The crystallite size calculated for $Bi_xEu_{0.05}Y_{0.95-x}PO_4$ (x = 0.02, 0.05, 0.07, and 0.10) at different annealing temperatures was in the range of 21−36 nm. XRD diffraction patterns of $Bi_xEu_{0.05}Y_{0.95-x}PO_4$ (x = 0.05, 0.07, and 0.10) also show a transformation from the hydrated hexagonal to dehydrated tetragonal phase with increasing annealing temperatures as shown in Figure S1 (see the Supporting Information).

Zollfrank et al.[4] also reported a phase transformation from hydrated europium(III) orthophosphate ($EuPO_4 \cdot n H_2O$) of hexagonal crystal structure to monoclinic nonhydrated $EuPO_4$ at 600 °C. In an earlier work,[10] it has been shown that the phase transformation from hydrated hexagonal to dehydrated monoclinic structure takes place in the temperature range of 200−230 °C. It is established that water molecules can be made stable up to a very high temperature (800−900 °C) in such compounds. When the concentration of Bi^{3+} ion increases, the relative peak intensity of the (102) plane with respect to the highest peak (111) plane increases. Also, in all 500 and 700 °C heated samples, the peak intensity variation in (111) and (102) planes is marginal. Figure S2 (see the Supporting Information) shows the XRD patterns of 900 °C annealed samples of YPO_4 codoped with Eu^{3+} and Bi^{3+}.

2.2. TGA and DTA Studies. Thermogravimetric analysis (TGA) and differential thermal analysis (DTA) were utilized to analyze the thermal properties of $Bi_{0.02}Eu_{0.05}Y_{0.93}PO_4$ as shown in Figure 2a. The initial weight loss of 2% in TGA curve below 200 °C, accompanied by an endothermic peak at 184 °C, is assigned to the loss of water molecules present on the surface of the sample.[1] The crystal structural transformation from hexagonal phase (hydrated) to tetragonal phase (dehydrated) as presented in the preceding section is observed as a sharp exothermic peak at 889 °C. The slight difference in phase transition is due to the difference in the duration of annealing at particular temperature. It is to be noted that the apparent increase in weight (TGA curve) above 600 °C is due to instrument artifact.

dx.doi.org/10.1021/ja1092437 |J. Am. Chem. Soc. 2011, 133, 2998–3004

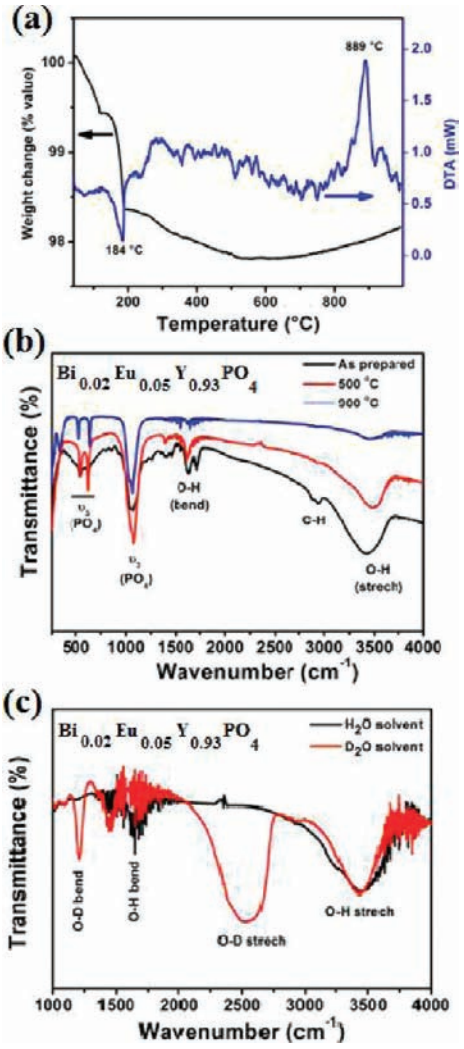

Figure 2. (a) TGA/DTA and (b) IR spectra of $Bi_{0.02}Eu_{0.05}Y_{0.93}PO_4$ (prepared with PEG and EG) at different annealing temperatures and (c) IR spectra of $Bi_{0.02}Eu_{0.05}Y_{0.93}PO_4$ (prepared without PEG and EG) in different solvents (H_2O and D_2O).

2.3. IR Study. Figure 2b shows the IR spectra of $Bi_{0.02}Eu_{0.05}Y_{0.93}PO_4$ at different annealing temperatures (as-prepared, 500 and 900 °C) prepared with PEG and EG. All the analyzed samples show the typical peaks of $(PO_4)^{3-}$ at 526 and 647 cm^{-1}, attributed to bending vibrations commonly known as the ν_4 region,[11] and strong bands centered at 1110 and 1077 cm^{-1} merged together, corresponding to stretching vibrations generally known as the ν_3 region.[12] Peaks correspond to bending and stretching vibrations, for the O−H group as well as the stretching vibrations of H−C−H groups are also observed. The reduction in the intensity of the O−H vibration in the 900 °C heated $Bi_{0.02}Eu_{0.05}Y_{0.93}PO_4$ further confirms the transition from a hexagonal hydrated to a tetragonal dehydrated phase. Figure 2c shows IR data of $Bi_{0.02}Eu_{0.05}Y_{0.93}PO_4$ prepared in D_2O and H_2O solvents in the absence of capping agent PEG and EG. Only the data range 1000−4000 cm^{-1} is shown to see their vibration absorptions. The stretching vibration of O−D is observed around 2500 cm^{-1}, which is less than that of O−H (3450 cm^{-1}).

2.4. TEM Study. Figure 3a shows the transmission electron microscopy (TEM) image of the 500 °C annealed $Bi_{0.02}Eu_{0.05}Y_{0.93}PO_4$. Nanorods having diameter of 15 nm and length of 0.2−0.8 μm can be observed. The left column of Figure 3 shows the full length view of nanorod bundles and the selected area electron diffraction (SAED) image of the sample, which represents a well-crystalline sample. The 900 °C heated sample shows various shapes of nanoparticles (the right column of Figure 3). When the annealing temperature is increased to 900 °C, the nanorods become distorted and break up into smaller particles, as can be seen in Figure 3D. Numbers of pores or holes could also be observed in the distorted nanorods. The SAED study (Figure 3E, F) shows that the sample is well crystalline. The emergence of pore or holes along with the distortion of nanorods could be due to the voids left by the loss of water molecules when the hexagonal hydrated phase changes to the tetragonal dehydrated phase as discussed earlier. In our earlier work on Ce^{3+} codoped YPO_4:Eu^{3+}, we observed a similar transformation of the nanorods to disoriented nanoparticles as well as the emergence of pores with heat treatment.[2] The transformation occurs in the temperature range of 800−900 °C in $Ce_xEu_{0.05}Y_{0.95-x}PO_4$, but in the present study, it is observed in the 700−800 °C temperature range.

2.5. Photoluminescence Study. *2.5.1. Excitation and Emission Studies.* Figure S3 (see the Supporting Information) shows the excitation and emission spectra of as-prepared $Eu_{0.05}Y_{0.95}PO_4$ nanoparticles. In the excitation spectra monitoring the emission at 593 nm, a broad peak centered at 250 nm is observed which is attributed to the Eu−O charge transfer band (CTB). This arises from the transition of 2p electrons of O^{2-} to the empty 4f orbitals of Eu^{3+} ions. We could also observe peaks at 318, 362, 376/381, and 395 nm, which correspond to $^7F_{0,1}\rightarrow{}^5H_{3,6}$, $^7F_{0,1}\rightarrow{}^5D_0$, $^7F_{0,1}\rightarrow{}^5G_1$,$^5L_7$, and $^7F_0\rightarrow{}^5L_6$ transitions of Eu^{3+}, respectively.[8] The emission spectrum of as-prepared $Eu_{0.05}Y_{0.95}PO_4$ nanoparticles excited at 395 nm shows the peaks of Eu^{3+} at 593 and 618 nm corresponding to the magnetic dipole transition ($^5D_0\rightarrow{}^7F_1$) and electric dipole transition ($^5D_0\rightarrow{}^7F_2$), respectively.[8] Also, emission peaks at 650 and 697 nm are observed.

Figure 4a shows the emission spectra of $Bi_xEu_{0.05}Y_{0.95-x}PO_4$ (x = 0, 0.02, 0.05, 0.07, and 0.10) when excited at 395 nm. To compare the luminescence intensity, the area under the magnetic and electric dipole transitions was measured by fitting with Gaussian distribution function. All the fittings were carried out in the range of 580−605 and 605−630 nm for magnetic ($^5D_0\rightarrow{}^7F_1$) and electric dipole ($^5D_0\rightarrow{}^7F_2$) transitions, respectively. The integrated areas for the magnetic and electric dipole transitions of Eu^{3+} as well as their full widths at half-maximum (fwhm) for the $Bi_xEu_{0.05}Y_{0.95-x}PO_4$ (x = 0.02, 0.05, 0.07, and 0.10) at different annealing temperatures (as-prepared, 500, 700, 800, and 900 °C) have been summarized in Table S2 (see the Supporting Information). The luminescence intensity of Eu^{3+} decreases suddenly with increase of the Bi^{3+} codopant concentrations. Above x = 0.2, luminescence intensity is almost constant. The decrease of the luminescence intensity is mainly due to the presence of the H_2O, which is an efficient luminescent quencher through multiphonon relaxation. There is a slight increase in the luminescence intensity at excess Bi^{3+} codoping (10 at. %), which might be an effect from the formation of the new phase of $BiPO_4$ (as was also observed in the XRD study).

The presence of water molecules in the samples acts as primary centers of nonradiative transition. The rate of the nonradiative transition, R_0, is exponential and can be expressed as $R_0 = A\exp[-(\Delta E - 2h\nu_{max})B]$, where A and B are constants. ΔE is the difference in energy between the excited and ground states of Eu^{3+} ion. ν_{max} is the highest available vibrational mode of the

dx.doi.org/10.1021/ja1092437 |J. Am. Chem. Soc. 2011, 133, 2998–3004

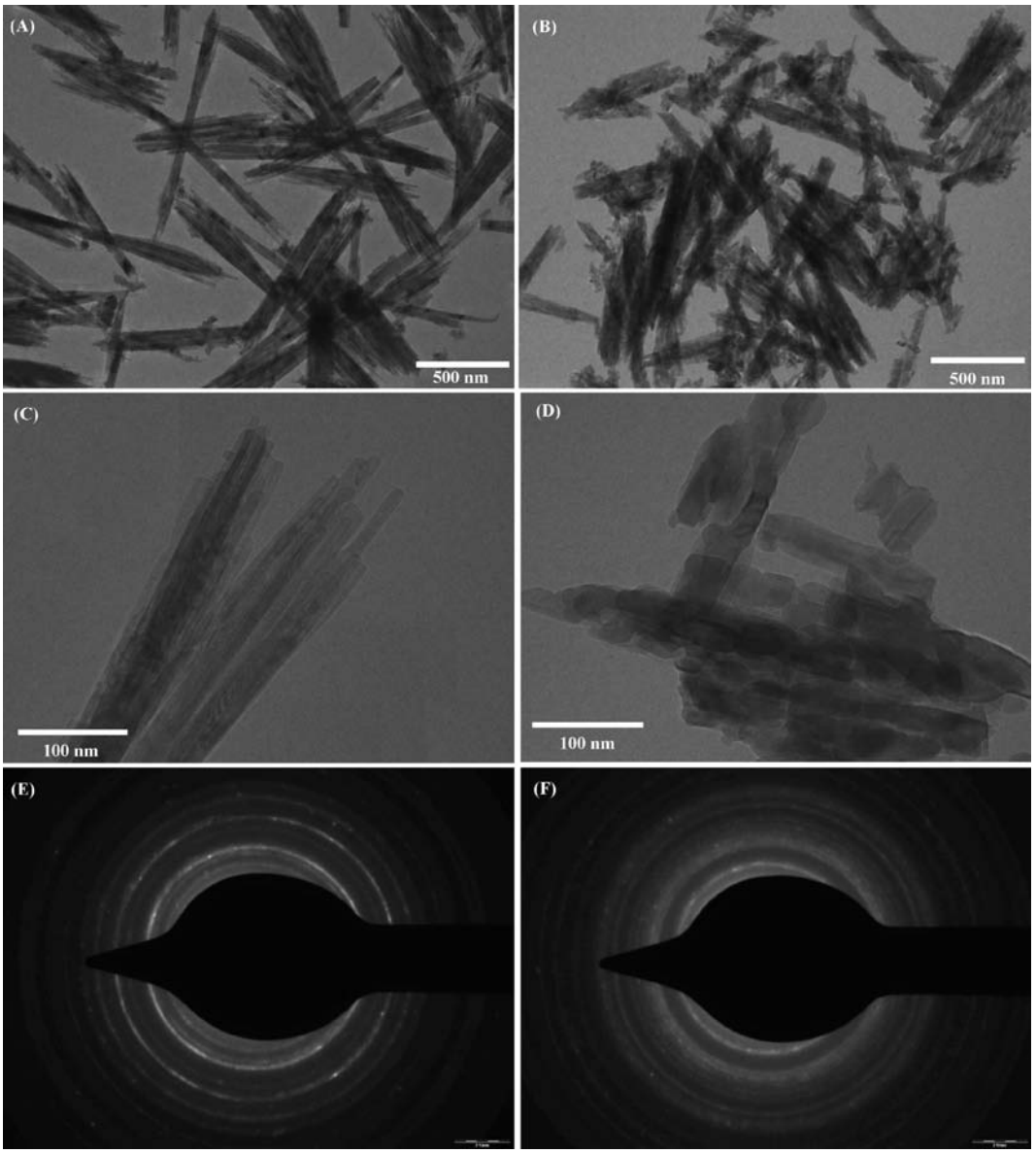

Figure 3. Images of 500 °C (left column) and 900 °C (right column) heated samples of $Bi_{0.02}Eu_{0.05}Y_{0.93}PO_4$ (prepared with PEG and EG): TEM images recorded at lower magnification (A,B) and higher magnification (C,D) and SAED (E,F).

surroundings of the rare earth ion. In Eu^{3+} ion, ΔE is about 10 000−15 000 cm^{-1}, and the value is comparable with the third/fourth overtone stretching vibration of the O−H group (3450 cm^{-1}). This O−H functional group arises from water molecules absorbed or associated with hexagonal structure. Now, the R_0 value becomes large because $\Delta E \approx 2h\nu_{max}$. This results in a (space) significant extent of nonradiative transfer of energy from the excited state of Eu^{3+} ion to the different vibration modes of O−H species, leading to the reduction in Eu^{3+} luminescence intensity. The nonradiative transfer of energy from excited states of Eu^{3+} to the surrounding phonons of O−H is termed as multiphonon relaxation. The rate of photon/energy loss is very fast ($<10^{-10}$ s), and it is associated with the nonradiative process.[13] Figure 4b shows emission spectra of $Bi_{0.02}Eu_{0.05}Y_{0.93}PO_4$ prepared in H_2O and D_2O solvents, and the excitation wavelength is fixed at 395 nm. This sample is prepared in the absence of EG and PEG. There is a ∼4-fold increase in the luminescence intensity when solvent H_2O is replaced by D_2O. Multiphonon relaxation is significantly reduced when the O−H vibration is replaced by O−D. The enhancement in luminescence is due to the extent of decrease in multiphonon relaxation.

Figure S4 (see the Supporting Information) shows the emission spectra of $Bi_xEu_{0.05}Y_{0.95-x}PO_4$ (x = 0.02, 0.05, 0.07, and 0.10) at different annealing temperatures. The excitation wavelength is fixed at 395 nm. Typical emission spectra of x = 0.02 are shown in Figure 4c. The spectra exhibit a typical emission peak of Eu^{3+} at 593 nm corresponding to the magnetic dipole transition ($^5D_0 \rightarrow {}^7F_1$) along with peaks at 618 and 697 nm corresponding to electric dipole transitions ($^5D_0 \rightarrow {}^7F_2$ and $^5D_0 \rightarrow {}^7F_4$), respectively. Apart from these, a weak emission peak centered at 650 nm corresponding to the $^5D_0 \rightarrow {}^7F_3$ transition is also observed. The luminescence intensity of the hydrated hexagonal phase (as-prepared, 500, and 700 °C annealed samples) is weak due to the presence of the luminescence quencher in the form of O−H group. There is a sudden emergence of Eu^{3+} emission peak for 800−900 °C, which was not observed until 700 °C. As stated

dx.doi.org/10.1021/ja1092437 |*J. Am. Chem. Soc.* 2011, 133, 2998–3004

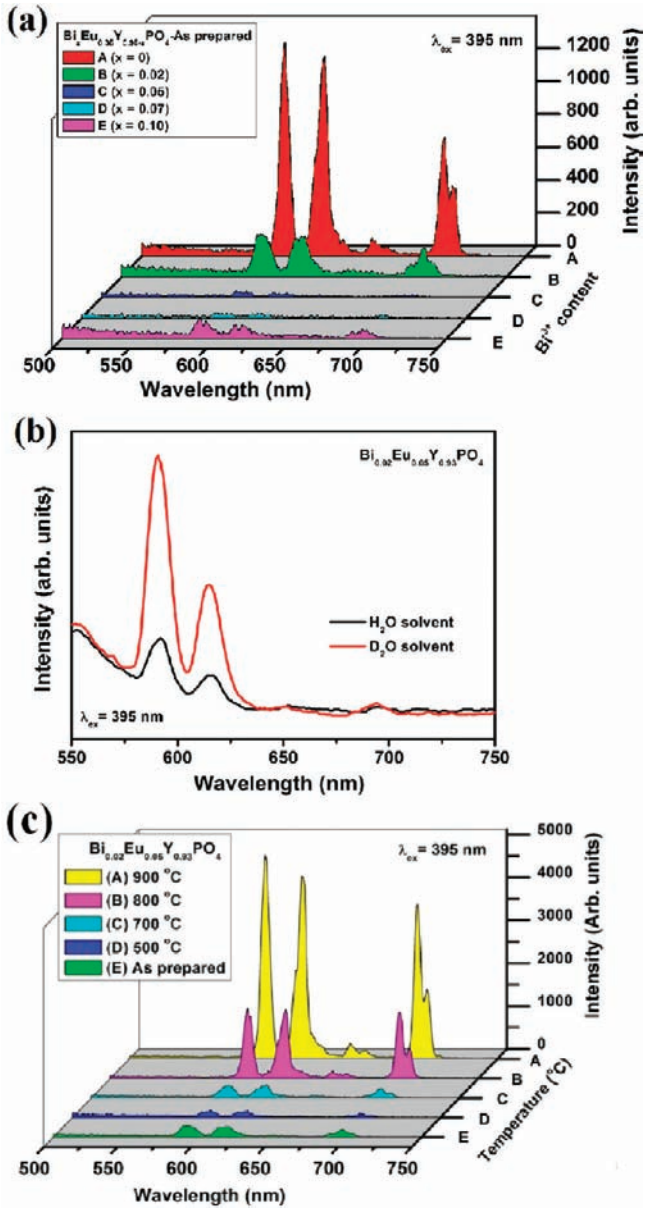

Figure 4. (a) Emission spectra of as-prepared $Bi_xEu_{0.05}Y_{0.95-x}PO_4$ (x = 0, 0.02, 0.05, 0.07, and 0.10) prepared in the presence of PEG and EG. (b) Emission spectra of $Bi_{0.02}Eu_{0.05}Y_{0.93}PO_4$ prepared in H_2O and D_2O solvents in the absence of PEG and EG. (c) Emission spectra of $Bi_{0.02}Eu_{0.05}Y_{0.93}PO_4$ (prepared in the presence of PEG and EG) heated at different temperatures.

above in the XRD studies, there is a phase transformation to dehydrated from hydrated phase as the temperature rises from 700 to 800−900 °C. The presence of O−H groups, which are efficient quenchers of luminescence through multiphonon relaxation,[2] present in the hydrated $Bi_xEu_{0.05}Y_{0.95-x}PO_4$ (x = 0.02, 0.05, 0.07, and 0.10) up to 700 °C heated sample, results in the loss of the luminescence intensity. It is noted that the recovery of luminescent intensity in the 800−900 °C heated sample is due to the loss of OH groups, which is confirmed by the crystal structure transformation from hydrated to dehydrated phase. For the 900 °C annealed samples of $YPO_4:Eu^{3+}$, luminescence intensity of Eu^{3+} has been found to improve after the codoping of Bi^{3+} (Figure 5). Here, the enhancement of the

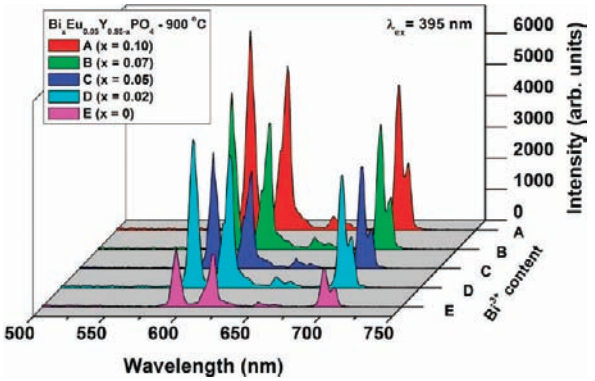

Figure 5. Emission spectra of $Bi_xEu_{0.05}Y_{0.95-x}PO_4$ (x = 0, 0.02, 0.05, 0.07, and 0.10) annealed at 900 °C.

luminescence intensity of the 900 °C heated Bi^{3+} codoped sample was observed. $YPO_4:Eu^{3+}$ is in the tetragonal phase for both the as-prepared and the annealed samples. Annealing the $YPO_4:Eu^{3+}$ at higher temperature (900 °C) does not enhance the emission intensity as much as compared to the annealed sample of the Bi^{3+} codoped $YPO_4:Eu^{3+}$. The enhancement of the emission intensity of the 900 °C annealed Bi^{3+} codoped sample is about 2−3 times that of the annealed $YPO_4:Eu^{3+}$.

The relative intensity ratio of $^5D_0 \rightarrow {}^7F_2$ to $^5D_0 \rightarrow {}^7F_1$ transitions can be used as a sensitive parameter for understanding the symmetry around the Eu^{3+} in the host material. This parameter is called the asymmetric ratio (I_{AS}). The intensity ratio I_{AS} for $Bi_xEu_{0.05}Y_{0.95-x}PO_4$ (x = 0.02, 0.05, 0.07, and 0.10) at different annealing temperatures (as-prepared, 500, 700, 800, and 900 °C) is found to be 1.00 ± 0.2 for all samples (Figure 6). This has been attributed to the equal occupancy of symmetric and asymmetric sites by Eu^{3+} ions in all the Bi^{3+} codoped $YPO_4:Eu^{3+}$ samples.

2.5.2. Lifetime Study. Figure 7a shows luminescence decay for $^5D_0$ level of Eu^{3+} in $Bi_xEu_{0.05}Y_{0.95-x}PO_4$ (x = 0, 0.02, 0.05, 0.07, and 0.10). Excitation and emission wavelengths are fixed at 395 and 593 nm, respectively. The intensity decreases with the increase in the Bi codopant content. Similar behavior has been observed in case of luminescence studies. Figure 7b shows the luminescence decay for the $^5D_0$ level of Eu^{3+} in $Bi_xEu_{0.05}Y_{0.95-x}PO_4$ (x = 0.02) samples annealed at different temperatures (as-prepared, 500, 700, 800, and 900 °C). The intensity improved after heat treatment, but significant improvement in the intensity is observed when the samples are annealed above 800 °C. Decay curves for emission for all the cases can be well-fitted into a biexponential function. Average lifetime values of as-prepared samples of x = 0 and 0.02 are found to be 2.7 and 1.7 ms, respectively. For x = 0.05−0.10, τ_{av} is found to be ∼0.5 ms. Lifetime values of 500, 700, 800, and 900 °C annealed samples of x = 0.02 are found to be 1.6, 2.3, 4.6, and 5.1 ms, respectively. This study will help in understanding the luminescence properties of hexagonal phase of other rare-earth phosphates so that the proper choice of heat-treatment temperature and activators/sensitizers will be optimized.

3. CONCLUSIONS

YPO_4 nanoparticles codoped with Eu^{3+} (5 at. %) and Bi^{3+} (2−10 at. %) have been synthesized by a simple coprecipitation method using a polyethylene glycol−glycerol mixture, which acts as capping agent. The incorporation of Bi^{3+} ions into the YPO_4:

dx.doi.org/10.1021/ja1092437 |J. Am. Chem. Soc. 2011, 133, 2998–3004

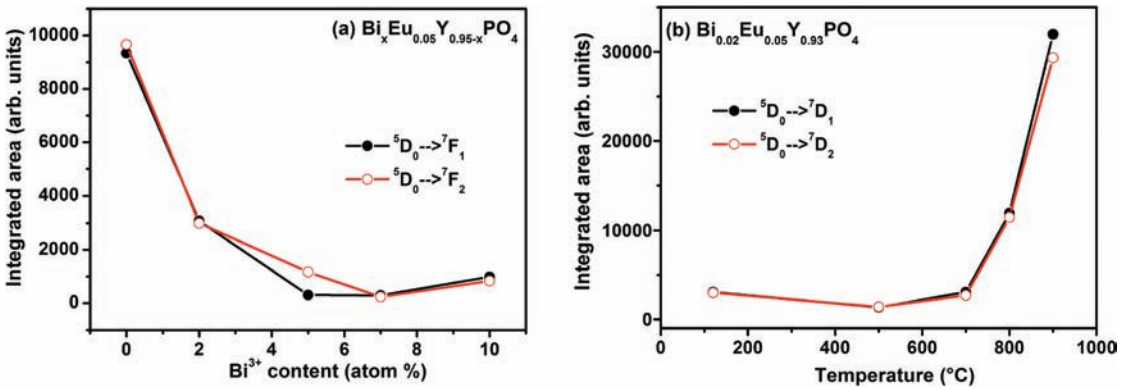

Figure 6. Integrated area of $^5D_0-^7F_1$ and $^5D_0-^7F_2$ transitions at an excitation wavelength of 395 nm at (a) different Bi^{3+} concentrations in $Bi_xEu_{0.05}Y_{0.95-x}PO_4$ and (b) different annealing temperatures in $Bi_{0.02}Eu_{0.05}Y_{0.93}PO_4$.

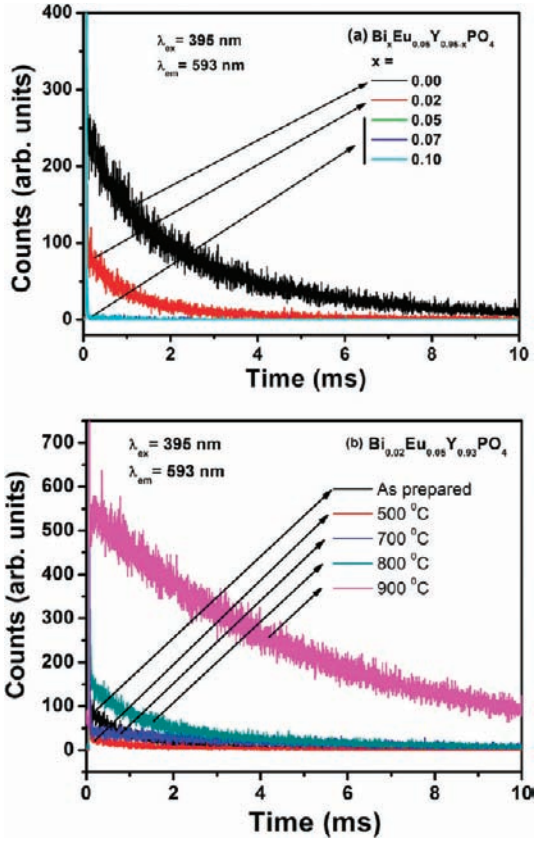

Figure 7. Decay curves for $^5D_0$ level of Eu^{3+} in (a) $Bi_xEu_{0.05}Y_{0.95-x}PO_4$ (x = 0.00, 0.02, 0.05, 0.07, and 0.10) and (b) $Bi_{0.02}Eu_{0.05}Y_{0.93}PO_4$ at different annealing temperatures (500, 700, 800, and 900 °C).

Eu^{3+} lattice induces a phase transformation from tetragonal to hexagonal and also a significant decrease in Eu^{3+} luminescence intensity. This is related to the association of the water molecules in the hexagonal phases of YPO_4 in which the nonradiative process from surrounding water molecules is dominating over the radiative process. Interestingly, luminescence intensity can be recovered after annealing above 800 °C in which the phase change from hexagonal to tetragonal structure takes place. Also, we observed that Bi^{3+} doping increases the luminescence intensity for the compounds as well as the distortion of the nanorods when annealed above 800 °C.

4. EXPERIMENTAL SECTION

4.1. Reagents and Materials. Yttrium(III) carbonate hydrate, $Y_2(CO_3)_3 \cdot xH_2O$ (99.9%), bismuth(III) nitrate pentahydrate, $Bi(NO_3)_3 \cdot 5H_2O$(99.9%), and ammonium dihydrogen phosphate, $(NH_4)H_2PO_4$-(99.999%), from Sigma-Aldrich, europium(III) oxide, Eu_2O_3 (99.9%), from Alfa Aesar, polyethylene glycol-1000 from Fluka, and glycerol, methanol, and hydrochloric acid were used as received without further purification. Deionized water was used throughout the experiment.

4.2. Synthesis of YPO_4:Eu^{3+}, Bi^{3+} Nanoparticles. *a. In H_2O Solvent.* $Bi_xEu_{0.05}Y_{0.95-x}PO_4$ (x = 0, 0.02, 0.05, 0.07, and 0.10) nanoparticles were synthesized by the polyethylene glycol−glycerol route. In a typical synthesis procedure of $Bi_{0.05}Eu_{0.05}Y_{0.90}PO_4$, stoichiometric amounts of $Bi(NO_3)_3 \cdot 5H_2O$ (0.106 g), Eu_2O_3 (0.038 g), and $Y_2(CO_3)_3$ (0.699 g) were dissolved in concentrated HCl in a 100 mL two-necked round-bottom flask, and excess acid was removed by evaporation with addition of water. The resulting transparent solution was allowed to mix with 10 g of polyethylene glycol-1000 (PEG) and 50 mL of glycerol and was heated at 80 °C for 30 min. To this reaction medium was added 0.5 g of $(NH_4)H_2PO_4$, and the solution was allowed to reflux at 120 °C for 2 h. The resulting white precipitate was collected by centrifuging at 10 000 rpm after washing with methanol. The precipitate was annealed at different temperatures (500, 700, 800, and 900 °C) for 4 h at ambient atmosphere. Similarly, other Bi codoped samples have been prepared. The atomic percentages (compositions) of $Bi_{0.05}Eu_{0.05}Y_{0.90}PO_4$ obtained at 900 °C were determined by energy dispersive X-ray (EDX) spectroscopy and found to be Bi = 0.7, Eu = 0.9, Y = 12.2, P = 17.2, and O = 68.7, and their theoretical atomic percentages are Bi = 0.8, Eu = 0.8, Y = 14.9, P = 16.6, and O = 66.8. Its EDX spectrum is shown in Figure S5 (see the Supporting Information).

b. In D_2O Solvent. In this procedure, we have prepared $Bi_{0.02}Eu_{0.05}$-$Y_{0.93}PO_4$ in D_2O solvent under an argon atmosphere. Stoichiometric amounts of the reactants $(Bi(NO_3)_3 \cdot 5H_2O$, Eu_2O_3, $Y_2(CO_3)_3)$ were dissolved in the minimum amount of concentrated HCl, and the excess HCl was removed by evaporation with addition of D_2O. The resulting solution was heated at 80 °C for 30 min under an argon atmosphere, and a stoichiometric amount of $(NH_4)H_2PO_4$ was added. The solution was refluxed at 120 °C for 2 h in D_2O medium.

4.3. Characterization of the Nanoparticles. A Philips X-ray diffractometer (PW 1071) with Cu K_α (1.5405 Å) radiation with an Ni filter was used for X-ray diffraction (XRD) study. All patterns were recorded over the angular range $10 \le 2\theta/\text{deg} \le 70$ with a step size of $\Delta 2\theta = 0.02$. The average crystallite size (t) was calculated using the Debye−Scherrer relation, $t = 0.9\lambda/\beta \cos\theta$, where λ is the wavelength of the X-ray and β is the full width at half-maximum (fwhm). The powder

dx.doi.org/10.1021/ja1092437 |J. Am. Chem. Soc. 2011, 133, 2998–3004

samples were ground and dispersed in methanol on a glass slide and allowed to dry.

Thermal analyses (TG/DTA) of as-prepared powder sample were carried out using a TG-DTA Instruments (SETARAM 92-16.18). The samples under examination were heated at a rate of 5 °C min^{-1} in argon atmosphere.

Infrared spectra were recorded on a FT-IR spectrometer (Bomem MB 102). Powder samples were studied by making thin pellets with KBr.

A CM-200 transmission electron microscope was used for recording TEM images. For the TEM measurement, the powder samples were ground and dispersed in methanol. A drop of the dispersed particles was put over the carbon-coated copper grid and evaporated to dryness at room temperature.

All the luminescence spectra and decay lifetimes were recorded using EDINBURGH instrument FLS920 equipped with 450 W xenon lamp and μs-Flash lamp (100 W). Powder samples were dispersed in methanol and spread over the quartz slide and dried at room temperature.

■ ASSOCIATED CONTENT

Supporting Information. Lattice parameters, unit cell volume, and crystallite size of $Bi_xEu_yY_{1-x-y}PO_4$ ($x = 0.00-0.10$, $y = 0.05$) at different annealing temperatures along with JCPDS card no. 11-0254 and 42-0082, integrated area and full width at half-maximum (fwhm) of the electric and magnetic dipole transitions of the emission spectra of $Bi_xEu_yY_{1-x-y}PO_4$ (x = 0.02, 0.05, 0.07, and 0.10, $y = 0.05$), XRD patterns of $Bi_xEu_yY_{1-x-y}PO_4$ (x = 0.05, 0.07, and 0.10, $y = 0.05$) at different annealing temperatures, XRD patterns of 900 °C annealed samples of YPO_4 codoped with Eu^{3+} and Bi^{3+}, excitation and emission spectra of $Eu_{0.05}Y_{0.95}PO_4$, photoluminescence spectra of $Bi_xEu_{0.05}Y_{0.95-x}PO_4$ at different annealing temperatures, and EDX spectrum of $Bi_{0.05}Eu_{0.05}Y_{0.90}PO_4$ obtained at 900 °C. This material is available free of charge via the Internet at http://pubs.acs.org.

■ AUTHOR INFORMATION

Corresponding Author
rsn@barc.gov.in

■ ACKNOWLEDGMENT

We thank Dr. T. Mukherjee, Chemistry Group, BARC and Dr. D. Das, Chemistry Division, BARC for their support and encouragement during this work and A. M. Parag, MSD, BARC for help in recording EDX spectra. M.N.L. thanks the University Grant Commission, New Delhi for providing the UGC Research Fellowship in Science for Meritorious Students.

■ REFERENCES

(1) (a) Bauer, E.; Mueller, A. H.; Usov, I.; Suvorova, N.; Janicke, M. T.; Waterhouse, G. I. N.; Waterland, M. R.; Jia, Q. X.; Burrell, A. K.; McCleskey, T. M. *Adv. Mater.* **2008**, *20*, 4704. (b) Meyssamy, H.; Riwotzki, K.; Kornowski, A.; Naused, S.; Haase, M. *Adv. Mater.* **1999**, *11*, 840. (c) Buhler, G.; Feldmann, C. *Angew. Chem., Int. Ed.* **2006**, *45*, 4864. (d) Li, Q.; Yam, V. W. *Angew. Chem., Int. Ed.* **2007**, *46*, 3486. (e) Yan, R.; Sun, X.; Wang, X.; Peng, Q.; Li, Y. *Chem.-Eur. J.* **2005**, *11*, 2183.

(2) Luwang, M. N.; Ningthoujam, R. S.; Jagannath; Srivastava, S. K.; Vatsa, R. K. *J. Am. Chem. Soc.* **2010**, *132*, 2759.

(3) Kijkowska, R. *Thermochim. Acta* **2003**, *404*, 81.

(4) Zollfrank, C.; Scheel, H.; Brungs, S.; Greil, P. *Cryst. Growth Des.* **2008**, *6*, 776.

(5) Wiberg, E.; Wiberg, N.; Holleman, A. F. *Inorganic Chemistry*; Academic Press: New York, 2001; p 1263.

(6) Park, W. J.; Yoon, S. G.; Yoon, D. H. *J. Electroceram.* **2006**, *17*, 41.

(7) Park, W. J.; Jung, M. K.; Im, S. J.; Yoon, D. H. *Colloids Surf., A* **2008**, *313−314*, 373.

(8) (a) Ningthoujam, R. S. *Chem. Phys. Lett.* **2010**, *497*, 208. (b) Singh, L. R.; Ningthoujam, R. S.; Sudarsan, V.; Srivastava, I.; Singh, S. D.; Dey, G. K.; Kulshreshtha, S. K. *Nanotechnology* **2008**, *19*, 055201. (c) Fang, Y. P.; Xu, A. W.; Song, R. Q.; Zhang, H. X.; You, L. P.; Yu, J. C.; Liu, H. Q. *J. Am. Chem. Soc.* **2003**, *125*, 16025.

(9) Bunzli, J. *Nat. Chem.* **2010**, *2*, 696.

(10) Di, W.; Wang, X.; Chen, B.; Lu, S.; Zhao, X. *J. Phys. Chem. B* **2005**, *109*, 13154.

(11) Kemp, W. *Organic Spectroscopy*; Macmillan: Hampshire, UK, 1975.

(12) (a) Begun, G. M.; Beall, G. W.; Boatner, L. A.; Gregor, W. J. *J. Raman Spectrosc.* **1981**, *11*, 273. (b) Yaiphaba, N.; Ningthoujam, R. S.; Singh, N. R.; Vatsa, R. K. *Eur. J. Inorg. Chem.* **2010**, 2682. (c) Phaomei, G.; Ningthoujam, R. S.; Singh, W. R.; Singh, N. S.; Luwang, M. N.; Tewari, R.; Vatsa, R. K. *Opt. Mater.* **2010**, *32*, 616.

(13) Yan, R.; Sun, X.; Wang, X.; Peng, Q.; Li, Y. *Chem.-Eur. J.* **2003**, *11*, 2183.